Highlights of Spanish Astrophysics VI, Proceedings of the IX Scientific Meeting of the Spanish Astronomical Society held on September 13 - 17, 2010, in Madrid, Spain. M. R. Zapatero Osorio et al. (eds.)

The infrared overluminosity of young, ultracool substellar objects

M. R. Zapatero Osorio[1], R. Rebolo[2,3,4], G. Bihain[5], V. J. S. Béjar[2,3], J. A. Caballero,[6] and C. Álvarez[2,7]

[1] Centro de Astrobiología (CSIC-INTA), Crta. de Ajalvir km 4, 28850 Torrejón de Ardoz, Madrid
[2] Instituto de Astrofísica de Canarias, Vía Láctea s/n, 38205 La Laguna, Tenerife
[3] Dpt. Astrofísica, Universidad de La Laguna, 38205 La Laguna,Tenerife
[4] Consejo Superior de Investigaciones Científicas (CSIC), Madrid
[5] Astrophysikalisches Institut Potsdam, An der Sternwarte 16, 14482 Postdam, Germany
[6] Centro de Astrobiología (CSIC-INTA), P.O. 78, 28691 Villanueva de la Cañada, Madrid, Spain
[7] Gran Telescopio de Canarias, La Palma

Abstract

Most young, ultracool substellar objects with spectral types later than M9 show very red mid-infrared colors up to 24 μm, significantly redder than expected for their optical and near-infrared spectral classifications. These objects have estimated ages and masses in the intervals 20–300 Myr and 12–35 times the mass of Jupiter, respectively. According to optical data, their atmospheres have low gravity and are rather cool with characteristic effective temperatures between 1300 and 2400 K, rather close to the temperatures of close-in giant planets around solar-type stars. We focus on the particular case of G 196-3 B, an L3-type substellar companion orbiting a young low-mass star. We discuss various physical scenarios to account for its reddish nature and conclude that a low-gravity atmosphere with enshrouded upper atmospheric layers and/or a warm dusty disk/envelope provides the most likely explanations.

1 Introduction

The characterization of brown dwarfs and planetary-mass objects of known distance, metallicity, and age can provide critical tests for evolutionary models as well as empirical references for understanding the substellar population in the field, including planets orbiting stars. Confirmed members of nearby open star clusters and substellar companions to stars and massive

brown dwarfs can become good targets to establish the properties of benchmark objects. Among them, those located at the nearest distances are preferred since brown dwarfs and planets are intrinsically faint and they evolve toward lower luminosities with age (see [9, 4, 2]).

One ultracool substellar companion to a nearby low-mass star is G 196–3 B, found by direct imaging and proper motion studies at a separation of $\sim 16''$ from the active M2.5 star G 196–3 A [23]. In the discovery paper, the authors discussed that this system is young with an age in the interval 20–300 Myr. The young limit is imposed by the lack of the lithium absorption feature at 670.8 nm [6] in the optical spectrum of the primary star, implying that G 196–3 A has efficiently depleted this element by nuclear reactions. This happens at ages $\geq$20 Myr for the mass and temperature of this particular star. The intense emission lines like Hα and other activity properties, particularly the X-ray and UV emission of the M2.5 star, are quite similar to α Persei and Pleiades stars of the same temperature, suggesting that G 196–3 could have a likely age of about 100 Myr. [12] imposed a conservative upper limit of 640 Myr to the age of G 196–3 A based on the intensity of the most relevant chromospheric emission lines. More recently, [25] have reviewed the age of G 196–3 A and have set it at 25–300 Myr.

Since its discovery and due to its relative brightness (J = 14.8 mag), G 196–3 B has been observed spectroscopically at optical and near-infrared wavelengths by several groups. G 196–3 B is a moderate rotator ($v \sin i$ = 10 km s^{-1}), with no Hα emission [20]. Its rotation rate is quite similar to the rotational velocity of the primary star ($v \sin i$ = 15 km s^{-1}, [12]). The lithium feature is seen with a relatively strong intensity (a few to several Angstroms, [23, 19, 13]), strongly supporting its substellar nature. In addition, G 196–3 B displays all spectroscopic hallmarks of a low gravity atmosphere, thus confirming a young age. More recently, [7] has compared the optical spectrum of G 196–3 B to other field dwarfs of similar temperature and spectroscopic properties, and have assigned a spectral type of L3, slightly cooler than the L1 given in [19] and the L2 measured by [13]. As estimated in [23], the mass of G 196–3 B is 25^{+15}_{-10} times that of Jupiter.

Here we summarize some of the results presented in [32] focused on the description and interpretation of the photometric properties of G 196–3 B from the visible to the mid-infrared wavelengths (0.6–24 μm). For a wide description of data acquisition and analysis we refer to [32].

2 Red colors

Various authors have reported the finding of tens of ultracool dwarfs (objects with optical and near-infrared spectral types later than M7) whose optical spectra show unusual features, like weak FeH molecular absorption, weak K I and Na I doublets, and Li I absorption [7, 1, 23]. These are attributable to low-gravity atmospheres, indicating that those dwarfs are likely young ($\leq$ 300 Myr), low-mass brown dwarfs. Surprisingly, the great majority of these sources display redder near- and mid-infrared colors than what is expected from their spectral classification. Figure 1 illustrates such property, which is quite noticeable for the L dwarfs. This highly contrasts with their optical colors, which mimic rather well those of high-gravity

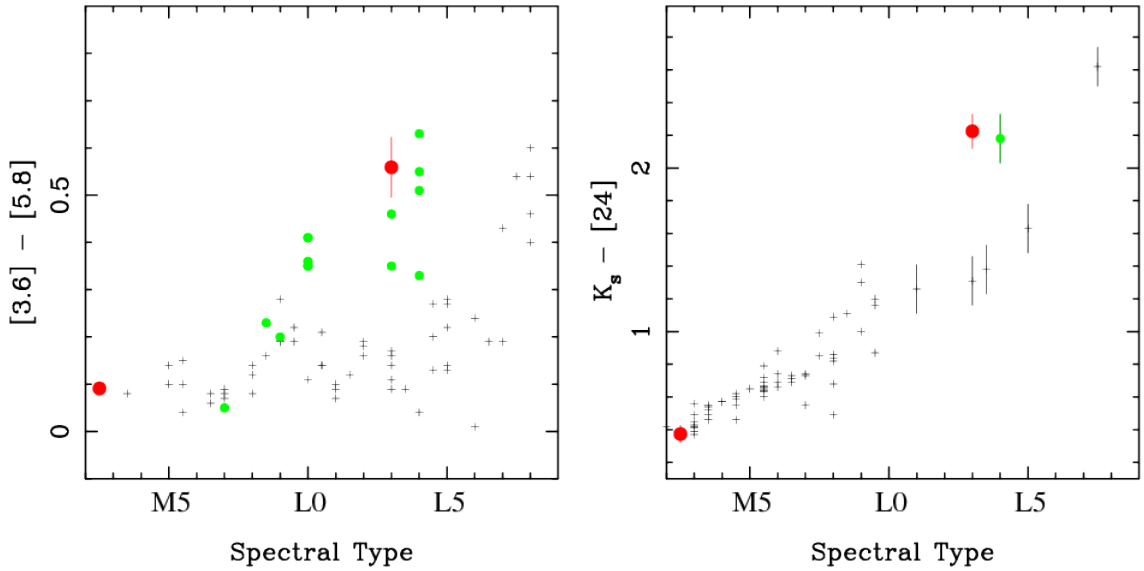

Figure 1: *Spitzer*/IRAC/MIPS photometry of field M and L dwarfs (crosses) is provided by [22, 11, 32]. The photometry of the young field dwarfs (green dots) is taken from [18, 1, 32]. The two members of G 196–3 are plotted as the red dots.

dwarfs in the field. The so far identified young L-type objects represents less than 10% of the total population of L dwarfs in the solar neighborhood.

None of these young sources are located near known star clusters with ages below 10 Myr, suggesting that they all have older ages. Furthermore, early-L dwarfs members of very young clusters like Upper Sco (∼5 Myr; [16]) and σ Orionis (∼3 Myr, [31, 5]), for which evolutionary models predict low surface gravities ($\log g \leq 4$ dex), do not show colors deviating significantly from the "high-gravity" field (the only exception we are aware of is the L0 object recently discovered in the Taurus association by [18]). This suggests that a low-gravity atmosphere may not be enough to account for all of the observed photometric properties.

3 G 196–3 B

Among the sample of field, young ultracool dwarfs there is G 196–3 B. We can take advantage of the existence of a primary star to constrain the metallicity, age and distance to the substellar object. This contrasts with the unknown parameters for the remaining young sources in the field. Photometric and spectroscopic properties of the star and the substellar object are given in Table 1. The most striking observable property of the overall spectral energy distribution (SED) of G 196–3 B is its apparent overluminosity at near- and mid-infrared wavelengths (see Fig. 2), which translates into colors redder than expected for its optical and near-infrared spectral type. We propose the following explanations, one or various of which may account for this signature: different metallicity, low-gravity atmosphere, a dust-

Table 1: Photometric and astrometric data of the G 196–3 system.

Parameter	G 196–3 A	G 196–3 B	Parameter	G 196–3 A	G 196–3 B
Spectral Type	M2.5	L3 ± 1	[4.5] (mag)	6.99 ± 0.01	11.47 ± 0.04
r (mag)[a]		22.44 ± 0.20	[5.8] (mag)	6.94 ± 0.01	11.10 ± 0.06
i (mag)		19.88 ± 0.03	[8.0] (mag)	6.93 ± 0.01	10.83 ± 0.04
z (mag)		17.83 ± 0.02	[24] (mag)	6.83 ± 0.05	10.55 ± 0.10
J (mag)[b]	8.08 ± 0.02	14.83 ± 0.05	$m_{\rm bol}$ (mag) [c]	9.85 ± 0.10	16.00 ± 0.10
H (mag)	7.41 ± 0.02	13.65 ± 0.04	$T_{\rm eff}$ (K)	3480 ± 90	1870 ± 100
K_s (mag)	7.20 ± 0.02	12.78 ± 0.03	$\mu_\alpha \cos\delta$ (mas/yr)	−142.3 ± 0.6	−144 ± 2
[3.6] (mag)	7.03 ± 0.01	11.66 ± 0.02	μ_δ (mas/yr)	−197.0 ± 0.9	−190 ± 20

[a]Sloan (DR7) photometry.
[b]2MASS photometry.
[c]See details in [32].

enshrouded atmosphere, continuum emission from a "hot" disk or dusty envelope, and the presence of a cool, unresolved companion.

Theory of model atmospheres predicts that metallicity and gravity impacts the colors of ultra-cool dwarfs, e.g., [14]. Reducing the metallicity increases the importance of molecular hydrogen collision-induced absorption in the infrared, producing blue colors. This is clearly observed in subdwarfs with L spectral classification, e.g., [3, 8]. G 196–3 B shows an opposing behavior, suggesting that it might have a metal-rich atmosphere. These atmospheres are also dustier. The optical spectrum of G 196–3 A (the star) is very similar to standard M2–M3 stars, including the solar-metallicity Pleiades and α Persei stellar members, see [23]. Furthermore, the great majority of nearby stars have nearly solar composition [21, 29]. From theoretical model atmospheres, metal-rich ultracool dwarfs have redder 1–4 μm colors than solar-metallicity dwarfs while the 5–15 μm spectrum does not change significantly [27], which contrasts with the properties of G 196–3 B. Therefore, high metallicity cannot explain the infrared overluminosity of G 196–3 B.

In ultra-cool dwarfs, decreasing the atmospheric gravity or gas density has a qualitatively similar effect on the photospheric gas pressure and chemistry of gas and condensates as increasing the metallicity [15]. Low gravities tend to produce red infrared colors. G 196–3 B displays all the spectroscopic hallmarks typically used to recognize low-gravity objects. Furthermore, from kinematic considerations its age is likely younger than the Pleiades, thus supporting a low-gravity atmosphere. Evolutionary models predict a surface gravity in the range $\log g = 4.1$–4.7 dex for G 196–3 B, which compares to the higher values ($\log g \sim 5$ dex) of older dwarfs of similar types. No model reproduces the very red colors of G 196–3 B.

The observed optical and infrared SED of G 196–3 B can be modeled by combining the emissions of an object with the same energy distribution than field L2–L3 dwarfs scaled to fit the J-band flux of the target and an additional source emitting like a single temperature black body. The L2–L3 dwarf component would mostly account for the visible up to the near-

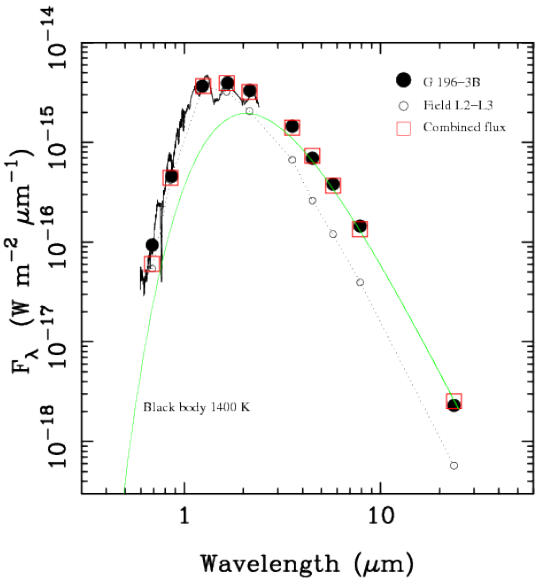

Figure 2: Spectral energy distribution (SED) of G 196–3 B is shown with a solid line (optical and near-infrared spectrum) and black solid circles. The average SED of L2–L3 field dwarfs is depicted with dotted line and open circles. The green solid line denotes the 1400-K black body emission 4 times less luminous than the brightness of G 196–3 B in the J-band (1.2 μm). The combined black-body and the L2–L3 SED is plotted as red open squares.

infrared fluxes, while the "black body" source would contribute notably to the mid-infrared fluxes. We found that a black body of 1400 K with a J-band flux four times fainter than that of the L2–L3 dwarf provides a reasonable fit to the thermal emission of the substellar object. Slightly cooler black bodies produce larger fluxes at red wavelengths while warmer ones yield insufficient emission. Figure 2 illustrates our results. The agreement between the SED of G 196–3 B and the modeled SED is within 1–2 σ uncertainty for the I through [24] passbands, while the R-band is not well reproduced. No combination of L2–L3 dwarfs and observed SEDs of cooler field dwarfs (e.g., L2–L3 + L7.5, L2–L3 + T1) provides a better match to G 196–3 B. The integrated luminosities of both the L2–L3 dwarf and the "black body" source are nearly equal even though their effective temperatures differ by about 500–700 K.

We may speculate that G 196–3 B is comprised of an L2–L3 component and a cooler companion with a characteristic temperature of 1400 K and a J-band flux four times lower than the L2–L3 dwarf. High spatial resolution images do not reveal G 196–3 B as a binary, so we can impose an upper limit of 0.3″ on the physical separation of both putative components. In the field, dwarfs of ∼2100 and ∼1400 K have bolometric luminosities differing by a factor of five. However, from our simple assumption we derived that both components show a luminosity ratio close to one, i.e., the cooler member should be 1.5 times larger in size than the warmer component. Substellar evolutionary models predict that objects with masses around the deuterium-burning mass limit (i.e., 0.012–0.02 $M_\odot$) and ages below ∼100–200 Myr must burn deuterium. During this stage, there is a "luminosity reversal" because these

objects become brighter than the inmediately more massive brown dwarfs and at least as luminous as 0.025–0.030 $M_\odot$ bodies. Therefore, for an age younger than ∼100–200 Myr, G 196–3 B might be formed by two objects with masses of 0.012–0.02 and 0.02–0.03 $M_\odot$ and similar luminosity. There is an issue, however, with the predicted surface temperatures and object sizes. The same evolutionary models assign similar temperatures and a nearly constant radius to both the deuterium-burning and non-burning bodies of these masses. This is not consistent with our modelization of G 196–3 B's SED, which suggests discrepant temperatures and sizes for the two putative members, undermining the probability of the multiplicity hypothesis.

Alternatively, the 1400-K black-body-like emission may result from an optically thick disk or envelope surrounding the central brown dwarf. [17, 24, 31] showed that a large fraction of brown dwarfs and free-floating planetary-mass objects harbor disks at ages below 10 Myr. These disks may evolve into debris disks in a manner similar to the disks of stars. The presence of a (debris) disk is compatible with the young age of G 196–3 B. More than 40% of the stars with $\leq$ 100 Myr display flux excesses at 24 μm due to the presence of debris disks [10]. However, "hot" dust is rare in stars older than ∼10 Myr, e.g., [26]. Regarding G 196–3 B, the ∼1400 K effective temperature of the disk warm dust implies that the bulk of the observed material lies in a narrow belt ∼1 radius from the brown dwarf, making this scenario unlikely.

One may think that the dense envelope has actually developed as a result of natural thermochemical processes in the upper atmospheric layers of G 196–3 B, which are producing dust grains small enough to be sustained in the photosphere. These would be responsible for the near- to mid-infrared reddening. The 1400-K characteristic temperature might be related to the $T_{\rm cr}$ parameter introduced by [28] in his model atmospheres, which essentially determines the thickness of the photospheric dust clouds or layers. Low values of $T_{\rm cr}$ imply very dusty (optically thick) atmospheres.

Another possibility is that the warm dusty disk around G 196–3 B may have appeared from "recent" and quite frequent stochastic events like episodes of high energy collisions among planetesimals (akin to the solar system's Late Heavy Bombardment and/or to the processes that are supposed to give rise to rocky planets, see review by [30]). In this scenario, the disk may be situated further away from the central object. This would suggest that even low-mass brown dwarfs are capable of forming planets through the same processes than more massive stars.

Any possibility previously discussed to account for the unusual red near- and mid-infrared colors of G 196–3 B can be also applied to the field young L dwarfs with related spectroscopic and photometric properties. Given the uncertainties associated to the models, we cannot firmly exclude any of the possibilities. However, a different metallicity seems to be the less likely explanation, while the effects on the output energy distribution driven by low gravity and enshrouded atmospheres and the presence of a warm dusty disk/envelope surrounding these objects remain as the most likely explanations. Follow-up radial velocity studies and polarimetric and high-resolution imaging will reveal whether these objects are multiple and/or harbor certain amounts of dust, which would help understand their nature.

References

[1] Allers, K. N., Liu, M. C., Dupuy, T. J., & Cushing, M. C. 2010, ApJ, 715, 561

[2] Baraffe, I., Chabrier, G., Allard, F., & Hauschildt, P. H. 1998, A&A, 337, 403

[3] Burgasser, A. J., et al. 2003, ApJ, 592, 1186

[4] Burrows, A., et al. 1997, ApJ, 491, 856

[5] Caballero, J. A., et al. 2007, A&A, 470, 903

[6] Christian, D. J., & Mathioudakis, M. 2002, AJ, 123, 2796

[7] Cruz, K. L., Kirkpatrick, J. D., & Burgasser, A. J. 2009, AJ, 137, 3345

[8] Cushing, M. C., et al. 2009, ApJ, 696, 986

[9] D'Antona, F., & Mazzitelli, I. 1994, ApJ Suppl., 90, 467

[10] Gáspár, A., et al. 2009, ApJ, 697, 1596

[11] Gautier, T. N. III, et al. 2007, ApJ, 667, 527

[12] Gizis, J. E., Reid, I. N., & Hawley, S. L. 2002, AJ, 123, 3356

[13] Kirkpatrick, J. D., et al. 2001, AJ, 121, 3235

[14] Leggett, S. L., et al. 2007, ApJ, 655, 1079

[15] Lodders, K., & Fegley, B., Jr. 2002, Icarus, 155, 393

[16] Lodieu, N., Hambly, N. C., Jameson, R. F., & Hodgkin, S. T. 2008, MNRAS, 383, 1385

[17] Luhman, K. L., Hernández, J., Downes, J. J., Hartmann, L., & Briceño, C. 2008, ApJ, 688, 362

[18] Luhman, K. L., Mamajek, E. E., Allen, P. R., & Cruz, K. L. 2009, ApJ, 703, 399

[19] Martín, E. L., et al. 1999, AJ, 118, 2466

[20] Mohanty, S., & Basri, G. 2003, ApJ, 583, 451

[21] Nordström, B., et al. 2004, A&A, 418, 989

[22] Patten, B. M., et al. 2006, ApJ, 651, 502

[23] Rebolo, R., et al. 1998, Sci, 282, 1309

[24] Scholz, A., & Jayawardhana, R. 2008, ApJ, 672, L49

[25] Shkolnik, E., Liu, M. C., & Reid, I. N. 2009, ApJ, 699, 649

[26] Silverstone, M. D., et al. 2006, ApJ, 639, 1138

[27] Stephens, D. C., et al. 2009, ApJ, 702, 154

[28] Tsuji, T. 2002, ApJ, 575, 264

[29] Valenti, J. A., & Fischer, D. A. 2005, ApJ Suppl., 159, 141

[30] Wyatt, M. C. 2008, ARA&A, 46, 339

[31] Zapatero Osorio, M. R., et al. 2007, A&A, 472, L9

[32] Zapatero Osorio, M. R., et al. 2010, ApJ, 715, 1408